Effect of Composition of (x)rGO/TiO_2 as Photoanode on the Performance of Dye Sensitized Solar Cells

Nabila Hari Arimbi[1], Nasikhudin[1,3(✉)], Markus Diantoro[1,3], Arif Nur Afandi[2], Herlin Pujiarti[1,3], and Adisria Marise Afianti[1]

[1] Departement of Physics, Faculty of Math and Natural Science, Universitas Negeri Malang, Jl. Semarang 5, Malang 65145, Indonesia
nasikhudin.fmipa@um.ac.id

[2] Departement of Electrical Engineering, Faculty of Engineering, Universitas Negeri Malang, Jl. Semarang 5, Malang 65145, Indonesia

[3] Centre of Advance Materials for Renewable Energy, Universitas Negeri Malang, Jl. Semarang 5, Malang 65145, Indonesia

Abstract. DSSC is a permanent alternative energy device in the form of environmentally friendly photoelectrochemical as a renewable energy source. So, the Efficiency of DSSC is still varied and relatively low. Therefore, in this study, a study was conducted on the effect of the composition of rGO/TiO_2 as a photoanode on the performance of DSSC. This research was carried out in four stages, namely deposition of blocking layer BL-1 with spin coating method, manufacture of mesoporous (x)rGO/TiO_2 composite by screen printing method with (x)rGO mass of immersion of thin film (x)rGO/TiO_2 with dye, and fabrication of DSSC. The characterization used in this research is X-Ray Diffractometer (XRD) to determine the crystal phase, crystal size, and crystal structure, Scanning Electron Microscope-Energy Dispersive X-Ray (SEM-EDX) to determine the surface morphology and constituent elements of the sample, Fourier Transform Infra-Red (FTIR) to determine the functional groups, UV-Vis, and I-V tests to determine the optical properties and performance of DSSC. The XRD data analysis of the sample (x)rGO/TiO_2 showed that the TiO_2 in the sample had a tetragonal crystal system rutile phase. The SEM results showed that the morphology of the (x)rGO/TiO_2 film was porous with the highest porosity of 83% so that it could increase dye absorption. Based on the UV-Vis results, the lowest band gap energy was 3.21 eV. DSSC performance based on the results of the I-V test analysis showed increased Efficiency if the concentration of rGO also increased, with the highest Efficiency of 1.16%.

Keywords: DSSC · Photoanode · Titanium Oxide · reduced Graphene Oxide

1 Introduction

In this era, the need for energy for society continues to increase, and fossil energy does not always meet these needs [1]. Thus, renewable energy sources are needed as a way out in addition to the use of fossil energy [2]. Solar cells can be developed as a

A. Doyan et al. (Eds.): ICSES 2022, APR 8, pp. 86–97, 2023.
https://doi.org/10.2991/978-94-6463-232-3_10

renewable energy technology [3]. Solar cells or photovoltaics are one of the devices that can be used to convert solar energy into electrical energy. Photovoltaics have efficiencies ranging from 6%-20% [4, 5].

With the development of solar cells to date, it has reached four generations. The first generation is crystal silicon-based solar cells, namely monocrystal solar cells with an efficiency between 16%-19% [6] and polycrystal solar cells with an efficiency of 13%-17% of the second generation, namely thin film solar cells [7], which have lower Efficiency compared to silicon-based solar cells, the Efficiency ranges from 6%-9% of the third generation, namely third generation solar cells [8]. Semiconductor-based organic solar with nanostructure materials, a combination of organic and non-organic materials [9], and the claim in the fourth generation is Perovskite Solar Cell with its light absorption system by organometallic halide, which makes higher Efficiency but with cheaper materials [10]. This type of organic solar cell is a Dye-Sensitized Solar Cell (DSSC). DSSC can be called Gratzel Cell because it was invented by O'Regan and Michael Gratzel in 1991 [3]. DSSC gets a lot of sympathy from the public because of its low price, easy fabrication, and high efficiency [11].

The DSSC structure comprises eight TiO_2 ori-plated materials as photoanode, dye as sensitizers, electrolytes, and counter electrodes [12]. Photoanodes are an essential component of DSSC because they have a function to store dye and can transfer electrons [13]. Binary metal oxide-based materials such as materials tested for photoanode use at DSSC [14]. Titanium Oxide semiconductor materials show as photoanode because they produce DSSC efficiency quite well in size nanoparticles TiO_2 have high chemical stability, can transfer electrons high, and have a binding energy of (60 meV) as well as the proper energy band structure for dye charge injection [15]. However, the crystal structure of TiO_2 electron mobility is low (0.1 – 4, causing recombination in the interface regions cm^2/Vs) in the photoanode layer [7, 21, 22]. In addition, modifications can also be made to the surface composted with TiO_2 Graphene Oxide (GO).

Graphene has good thermal, electrical, mechanical, and optical properties [16, 24]. Among various carbon-based materials, graphene and its derivative materials, such as reduced graphene oxide (rGO) and graphene oxide (GO), can be an option because they have good electrical and structural properties [1]. Using rGO-TiO2 composites as a photoanode in DSSC has been shown to increase solar cell efficiency by 30% of DSSC with pure nanoparticle photoanodes [18]. However, because it is difficult to obtain pure, conductive graphene, a similar material is used, namely graphene oxide (GO), which is then thermally reduced so that it becomes reduced graphene oxide (rGO) [19, 20]. DSSC with FTO/Photoanode/Dye/Electrolyte/PT configuration using organic dye from Germanium Flower produced the highest Efficiency of 0.00082% with an rGO wt concentration of 15%. This Efficiency is still very low. This study studied the effect of rGO- composition on DSSC performance. The DSSC configuration is TiO_2 FTO/TiO_2-rGO/dye-Ruthenium/electrolyte/Pt/FTO. In the study, the rGO layer will be deposited on and using TiO_2 Ruthenium N-719 dye and add Blocking Layer BL-1 to the substrate. Therefore, it is expected to be seen the influence of the composition of rGO-TiO_2 as a photoanade on its crystal structure, morphology, chemical bonds, optical properties, and Efficiency.

2 Method

In this process for washing the substrate is a beaker glass, disonicator, demineralized water, acetone, ethanol, multimeter, and hotplate. The first step is to clean the substrate with ethanol, put it on a beaker glass filled with soapy water, and condition the substrate to be submerged and sonicated for 15 min. Replace the water with demineralized water and sonicate for 15 min, and the substrate is drained with tissue. Then, heat the beaker glass containing acetone at 60C using a hotplate, rinse the substrate on the beaker glass, and dry it again with tissue. In the last step, we find the side with conductivity using a multimeter and attach a capton on the side of the conductive substrate.

We are repositioning the BL-1 Blocking Layer paste on the FTO substrate by using screen printing techniques (the size of the working area according to each characterization). Then spin the coating at a speed of 3000 rpm for 30 s. Finally, gradually heat the deposition substrate using a hotplate at 100 C, 300 C for 15 min, and 500 C for 30 min.

The manufacture of rGO-TiO_2 nanocomposites begin by dispersing 2 ml with rGO powder and dissolving using 0.5 ml of terpineol. The concentration of rGO against pastes with various powder masses is (5 wt%, ten wt %, 15 wt %). Furthermore, paste composted with rGO-TiO_2 is deposited on the FTO glass substrate using screen printing techniques. The layer deposited on the FTO is then heated using a hotplate at 100 C, 300 C for 15 min, and 500 C for 30 min in stages to produce nanoparticles which will then be used as a photoanode layer in the DSSC (Fig. 1).

FTO glass and counter electrode that uses (Pt/Au) in stacked stacking. Then, the FTO glass will be formed with a sandwich structure. The sandwich structure ensured that no air or water entered the DSSC sample. Using surlyn (Meltonix 117–250) is placed in a non-working area, with a thickness of 25 as a separator between the μm counter electrode and the photoanode. Pt/Au deposited FTO glass is used as a counter electrode on solar cells. Furthermore, the electrode layer is assembled with FTO glass coated with Pt/Au or counter electrode and then pressed using a sealing machine to form a small hole. The electrolyte (Mosaltye TDE-250) is injected or injected through the hole in the counter electrode using a special injection. After the electrolyte enters the solar cell, the cell to be tested is a vacuum. The standard DSSC structure in this study is FTO/BL/rGO-/TiO_2 dye/electrolyte/Pt/FTO. The DSSC cells that have been arranged are ready to be tested for electricity.

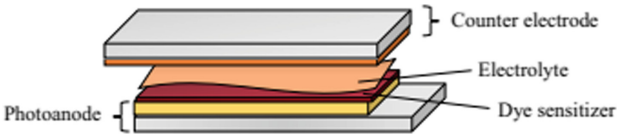

Fig. 1. Structure Divais DSSC

3 Results and Discussion

3.1 *rGO-TiO_2 Layer Microstructure*

The XRD test is carried out to determine the peak position; it can also identify the crystal structure or crystalline phase in the material by determining the lattice parameters to obtain the size of the crystals in the sample. XRD testing on DSSC was performed using a sample of which the deposition rGO-TiO_2 layer was patched up by FTO conductive. DSSC was tested to observe the phase of the structure formed on the working electrode. The results of the XRD test for various variations in rGO concentrations can be seen below:

The characteristic curve XRD is shown in Fig. 2, indicating that this sample has a TiO_2 rutile crystal phase corresponding to the Joint Committee on Powder Diffractions Standard (JCPDS) no 21–1276. The resulting crystal structure is also a TiO_2 rutile crystal phase with a tetragonal crystal system (lattice), with a space group I 41 / A M D with a group point of 4 / mmm. Diffraction peak $2\theta = 25.38°$, 26.49°, 37.79°, 47.22°, 51.55°, 61.66°, 65.59° with miller indices (002), (110), (101), (111), (210), (211) and (220). The comparison of the curve rGT01 to rGT05 peak peaks is almost no significant difference, as seen in Fig. 2.

In Table 1, it can also be seen the crystal size in the rGO- TiO_2 composite with each rGO concentration. The highest peak was taken from the XRD test results to obtain the crystal size. Determination of the crystal size using the approach of the Debye Scherrer equation. The rGO-TiO_2 spectrum shows TiO_2 the highest peak characteristics at $2\theta = 37.79°$, 37.77°, 37.30°, 37.76°, 37.78 with crystal sizes of ° 15.47 nm, 15.33 nm, 14.72 nm, 15.30 nm, and 15.42 nm, respectively. The five highest peaks identified indicate the compound is TiO_2 rutile dan, showing a peak rGO at $2\,\theta = 25.38$ with the miller index (002). (Peiris et al., 2018b). For the peak rGO, the crystallinity is lower than that

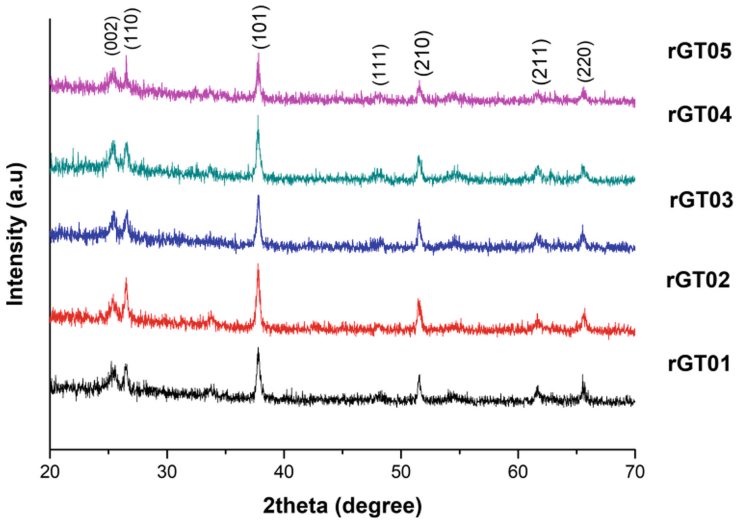

Fig. 2. XRD test results of rGO-TiO_2 composite samples

Table 1. FWHM Result Data and Crystal Size

Sample	FWHM (rad)	2theta	Crystal Size
rGT01	0,2362	37,79	15,47
rGT02	0,2362	37,77	15,33
rGT03	0,1968	37,30	14,72
rGT04	0,2362	37,76	15,30
rGT05	0,2755	37,78	15,42

of the linity crystal, indicating only one peak. The highest peak is found in FWHM of 0.2362 with an angle $2\theta = 37.79°$ and a crystalline size of 15.47 nm. In $rGT0_3$, the peak value decreases compared to other peaks, so the crystal size also decreases; it is because the sample can be contaminated with other impurities at the time of synthesis or testing, but the resulting composite is pure and crystallizes well because no peak diffraction of different compounds is detected.

3.2 *Morphology of Surface Layer rGO-TiO_2*

SEM testing was performed to determine the morphology of the rGO-TiO_2 surface layer. SEM results are obtained from images of morphological structures at certain magnifications. Morphological results for samples of each rGO variation TiO_2 can be seen in Fig. 2 with a magnification of 10000x.

Figure 3 is the morphology of a sample with a magnification of 10000x and looks like the layer on the surface of the sample undergoing several fragments of layers with a smaller particle distribution. It can also be observed to show that there are shown to be fine sheets with almost the same particle distribution size. The sheets from SEM characterization show the character traits of rGO according to the study results.

Figure 4, and morphology, it can be seen that composting rGO can cause clots in the sample. The clot (also called aggregation) can appear because when rGO is mixed with TiO2, those using terpineol solvents and the wet mixing process that may occur do not occur evenly. As a result of that phenomenon, particles that have the same charge are likely to gather into one group (group).

Because in this study, the mass of rGO-TiO_2 is varied and remains, the particles tend to be more significant to undergo aggregation (clumping). The analysis results were initiated by research reported by [1]. Different morphologies also give rise to different porosity values; the calculation of porosity values can be seen in Table 2 below the profit of each sample:

The data in Table 3 shows that the porosity value is increasing by 83%, indicating that the rGO-TiO_2 material is porous, which can increase dye absorption.

Furthermore, the results of the EDX (Energy Dispersive X-Ray) test are to determine the compounds or elements in the sample. The EDX results from each of the samples that have been synthesized are as follows:

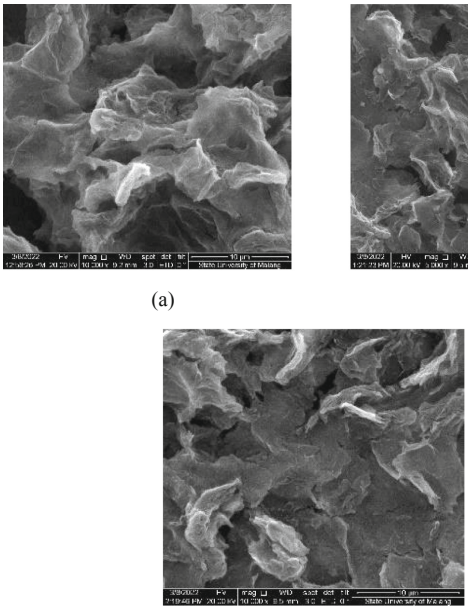

(a) (b)

(c)

Fig. 3. SEM micrograph for rGO/TiO_2 samples with each magnification of 10000x: (a) rGT01 (b) rGT02 (c) rGT03

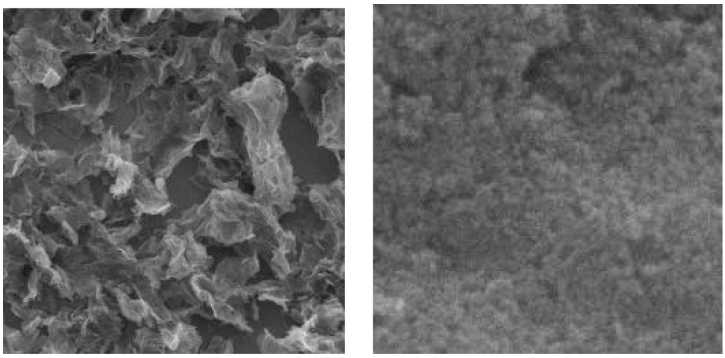

(a) (b)

Fig. 4. Surface morphology of rGO/TiO_2 with magnification differences: (a) magnification 5000x (b) magnification 50000x

Table 3 shows that the sample comprises titanium, oxygen, and carbon elements. At the same time, the percentage of atoms of titanium, carbon, and oxygen is different. The ratio of oxygen and titanium elements should be 1: 1 in each sample, but in the results of this test, it was found that the oxygen content was > 50%; this phenomenon is caused

Table 2. The porosity of each rGO-TiO_2 sample

Sample	Porosity (%)
rGT01	79%
rGT02	81%
rGT03	83%

Table 3. The constituent elements of each rGO-TiO_2 sample

Sample	Elements	Weight (%)	Atomic (%)
rGT01	C K	8,34	15,05
	O K	48,2	65,29
	Ti K	43,4	19,66
rGT02	C K	3,68	7,53
	O K	41,99	64,56
	Ti K	54,34	27,91
rGT03	C K	6,04	11,84
	O K	42,81	63,02
	Ti K	51,15	25,15

because there is an O that binds to C, like the results in the FTIR test, which produces C-O and C = O bonds.

3.3 Optical Properties of rGO-TiO_2

UV-Vis spectrophotometry is performed to determine the value of the absorbance spectrum to light and the band value of the energy gap. Spectrophotometric measurements that have been tested produce data in the form of absorbance values and wavelengths of light (wavelength). The spectrum of UV-Vis uptake in the rGO-TiO_2 sample can be seen in Fig. 5:

Figure 5 shows absorption by an intense transition in the UV Spectrum region, which is assigned to the absorption of the intrinsic band gap TiO_2, resulting from the electron transition from the valence band to the conduction band. Variations in rGO concentrations in composites significantly affect optical properties and increase the intensity of light absorption in the visible light region. The difference in absorbance intensity causes the band value of the energy gap to differ in the results of each sample. The determination of the band gap using the Touc Plot method is a straight line drawn between the multiplication of the absorbent energy and the coefficient absorbed against the photon (Lee et al., 2019) so that the gap band value in each sample can be seen in Table 4:

Based on Table 4, the data for the smallest energy gap was obtained at 3.21 eV and the largest at 3.43 eV. Then it can be said that the amount of rGO-TiO_2 concentration

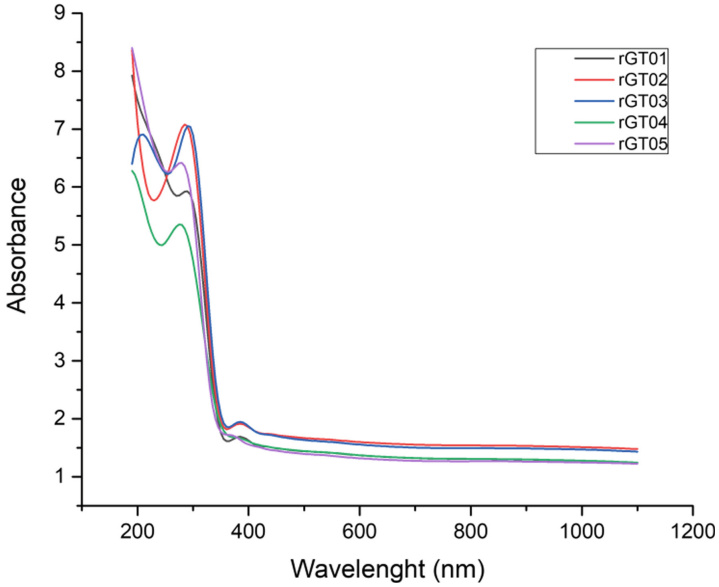

Fig. 5. UV-Vis Spectrum Curve for each rGO- TiO_2 sample mass

Table 4. Energy (h) band gap value in each sample

Sample	Energy gap (eV)
rGT01	3,21
rGT02	3,26
rGT03	3,38
rGT04	3,41
rGT05	3,43

affects the resulting band gap value. According to the literature results, the energy gap band in the anatase phase is 3.23 eV. The difference in the band gap results at the time of calculation and literature is because semiconductor materials are composted with rGO-TiO_2 with concentrations of various variations.

The distribution of gap band values with literature was also obtained by (Merazga et al., 2020) about the UV-Vis coating test to determine the band gap energy using the Touc Plot method, based on the results that reported a TiO_2 band gap energy value of 3.77 eV. In the data obtained, this study found the lowest n energy gap, which is very close to the band gap value in the TiO_2 anatase phase, which is 3.21 eV. The narrowed band gap can be attributed to the chemical bond between rGO due to the formation of the Ti-O-C bond.

3.4 *Effect of rGO-TiO_2 Composition on DSSC Performance*

Testing the electrical properties of DSSC to determine the electrical properties of the DSSC sample, namely the Fill Factor (FF) value, Jsc, Voc, and Efficiency () of the DSSC. These values can be known from the η current density (J) and voltage curve (V) obtained from the data for the parameters of the DSSC standard device cells that have been tested can be seen in Table 5:

From Table 5, it can be seen that Efficiency is increasing with the mass of rGO also increasing. So, it can be seen that with the addition of rGO of 2 wt %, 4 wt%, 6 wt %, 8 wt %, and 10 wt %, Efficiency will also increase. When the trend is depicted in a chart, it is as follows:

Figure 6, in tren above, was also obtained by previous studies that posited rGO-TiO_2 if the concentration of rGO increases, then Efficiency also increases. The phenomenon occurs because rGO-TiO_2 acts as a TiO_2 link of the porous layer. With the increase in the concentration of rGO-TiO_2 in, it can increase the surface area of the layer so that the impact can increase the ability of the working electrode to absorb, dye. Then the

Table 5. Solar cell divais parameters with various sample variations

Sample	J_{sc} (mA/cm^2)	V_{oc} (V)	P_{max} (mW)	FF	η (%)
rGT01	2,36	0,681	0,14	0,35	0,56
rGT02	2,40	0,568	0,18	0,32	0,73
rGT03	2,35	0,586	0,22	0,43	0,90
rGT04	2,48	0,589	0.27	0,38	1,10
rGT05	2,49	0,623	0,29	0,37	1,16

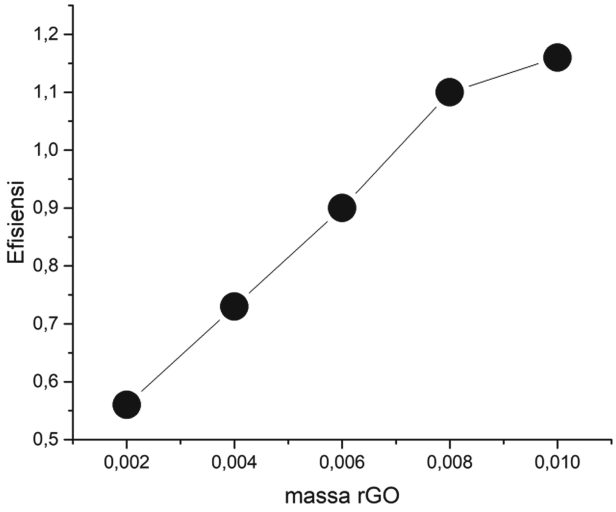

Fig. 6. Trend of adding rGO concentration to Efficiency in DSSC

sunlight captured by the dye will be more, and the Efficiency of the DSSC array will be significantly improved.

The case in the study (Lusi Safrani et al., 2021) based on the reported results for the results of current-voltage measurements, the addition of rGO-TiO_2 by 5wt% and the coating has increased the Efficiency of solar cells by 28% compared to purely as photoanodes. The presence of rGO-TiO_2 in this also contributes to an increase in photocurrent so that electron transfer becomes easier during irradiation and can suppress the recombination process in the layer interface.

4 Conclusion

A dye-sensitized solar cell based on rGO-TiO_2 composite has been fabricated. The addition of rGO in the TiO_2 can reduce the recombination of existing. rGO help optimize the transfer and charge separation process so that the greater the current generated. The result of SEM rGO-TiO_2 affects the stability and performance of DSSC, helping dye absorption due to its porosity. The results showed that the rGO-TiO_2 is a good material composite.

Acknowledgments. **T**hank you to the source of PNBP funds from the State University of Malang for supporting morally and materially and completing this paper.

References

1. AlShammari, A. S., Halim, M. M., Yam, F. K., & Kaus, N. H. M. (2020). Synthesis of Titanium Dioxide (TiO2)/Reduced Graphene Oxide (rGO) thin film composite by spray pyrolysis technique and its physical properties. Materials Science in Semiconductor Processing, 116(December 2019), 105140. https://doi.org/10.1016/j.mssp.2020.105140
2. Arsyad, W. S., Pristianti, A., Agusu, L., & Hidayat, R. (2019). RGO based photo-anode in dye-sensitized solar cells (DSSC) and its photovoltaic characteristics. IOP Conference Series: Materials Science and Engineering, 622(1). https://doi.org/10.1088/1757-899X/622/1/012008
3. Bukit, B. F., & Sirait, S. H. (2019). PREPARASI DISPERSI ANTIBAKTERI BERBAHAN DASAR TITANIUM DIOKSIDA (TIO 2) SERTA APLIKASINYA PADA KAIN DENGAN METODA DIP COATING Universitas Quality Berastagi Kasus Infeksi nosokomial di Indonesia meningkat setiap tahunnya . Salah satu penyebabnya ialah pe. 03(02), 640–644.
4. Diantoro, M., Maftuha, D., Suprayogi, T., Iqbal, M. R., Solehudin, Mufti, N., Taufiq, A., Hidayat, A., Suryana, R., & Hidayat, R. (2019). Performance of pterocarpus indicus willd leaf extract as natural dye TiO2-dye/ITO DSsC. Materials Today: Proceedings, 17, 1268–1276. https://doi.org/https://doi.org/10.1016/j.matpr.2019.06.015
5. Diantoro, M., Zaini, M. B., Suprayogi, T., Mufti, N., Zulaikah, S., & Hidayat, A. (2020). Effect of (SnO2:TiO2) nanoparticles on charging performance of integrated dye-sensitized solar cell-supercapacitor. AIP Conference Proceedings, 2231(April). https://doi.org/10.1063/5.0002438

6. Gupta, A., Sahu, K., Dhonde, M., & Murty, V. V. S. (2020). Novel synergistic combination of Cu/S co-doped TiO2 nanoparticles incorporated as photoanode in dye sensitized solar cell. Solar Energy, 203, 296–303. https://doi.org/https://doi.org/10.1016/j.solener.2020.04.043
7. He, X., Guo, Y., Liu, J., Li, X., & Qi, J. (2019). Fabrication of peanut-like TiO2 microarchitecture with enhanced surface light trapping and high specific surface area for high-efficiency dye sensitized solar cells. Journal of Power Sources, 423, 236–245. https://doi.org/https://doi.org/10.1016/j.jpowsour.2019.03.090
8. Hidayat, A., Setiadji, S., & Hadisantoso, E. P. (2019). Sintesis Oksida Grafena Tereduksi (rGO) dari Arang Tempurung Kelapa (Cocos nucifera). Al-Kimiya, 5(2), 68–73. https://doi.org/10.15575/ak.v5i2.3810
9. Himmah, S. W., Sa'Adah, U., Iswatin, A. D., Diantoro, M., Hidayat, A., & Supardi, Z. A. I. (2019). The Effect of Spin Coating Rotation on the Optoelectronic Properties of PANI/TiO2/FTO-Glass Photoanode. IOP Conference Series: Materials Science and Engineering, 515(1). https://doi.org/10.1088/1757-899X/515/1/012084
10. Liu, L., Zhang, Y., Zhang, B., & Feng, Y. (2017). A detailed investigation on the performance of dye-sensitized solar cells based on reduced graphene oxide-doped TiO2 photoanode. Journal of Materials Science, 52(13), 8070–8083. https://doi.org/10.1007/s10853-017-1014-9
11. Merazga, A., Al-Zahrani, J., Al-Baradi, A., Omer, B., Badawi, A., & Al-Omairy, S. (2020). Optical band-gap of reduced graphene oxide/TiO2 composite and performance of associated dye-sensitized solar cells. Materials Science and Engineering B: Solid-State Materials for Advanced Technology, 259(July 2018), 114581. https://doi.org/10.1016/j.mseb.2020.114581
12. Mohamadi Zalani, N., Koozegar Kaleji, B., & Mazinani, B. (2020). Synthesis and characterization of the mesoporous ZnO-TiO2 nanocomposite; Taguchi optimization and photocatalytic methylene blue degradation under visible light. Materials Technology, 35(5), 281–289. https://doi.org/https://doi.org/10.1080/10667857.2019.1678087
13. Moloto, W., Mafa, P. J., Mbule, P., Nxumalo, E., & Ntsendwana, B. (2022). Photoinduced electrochemical effect of porous BiPOM on TiO2 photoanode performance for dye-sensitized solar cells application. Materials Today Communications, 30. https://doi.org/10.1016/j.mtcomm.2021.103001
14. Nasikhudin, Diantoro, M., Kusumaatmaja, A., & Triyana, K. (2016). Preparation of PVA/Chitosan/TiO2 nanofibers using electrospinning method. AIP Conference Proceedings, 1755(July). https://doi.org/10.1063/1.4958575
15. Nipane, S. V., Lee, S. W., Gokavi, G. S., & Kadam, A. N. (2018). In situ one pot synthesis of nanoscale TiO2-anchored reduced graphene oxide (RGO) for improved photodegradation of 5-fluorouracil drug. Journal of Materials Science: Materials in Electronics, 29(19), 16553–16564. https://doi.org/https://doi.org/10.1007/s10854-018-9749-x
16. Nouri, E., Mohammadi, M. R., & Lianos, P. (2016). Impact of preparation method of TiO2-RGO nanocomposite photoanodes on the performance of dye-sensitized solar cells. Electrochimica Acta, 219, 38–48. https://doi.org/https://doi.org/10.1016/j.electacta.2016.09.150
17. PANGASTUTI, A. D. (2017). SINTESIS KOMBINASI ZnO-TiO2 DENGAN METODE SOL GEL SEBAGAI SEMIKONDUKTOR PADA DYE SENSITIZED SOLAR CELL (DSSC). Universitas Airlangga.
18. Peiris, D. S. U., Ekanayake, P., & Petra, M. I. (2018). Stacked rGO–TiO2 photoanode via electrophoretic deposition for highly efficient dye-sensitized solar cells. Organic Electronics, 59, 399–405. https://doi.org/https://doi.org/10.1016/j.orgel.2018.05.059
19. Rahman, M. F., Nasikhudin, Hidayat, A., & Diantoro, M. (2020). The influence of TiO2 film thickness in Dye-Sensitized Solar Cells (DSSC) performance based on TiO2/Ag@TiO2-ZnO. Journal of Physics: Conference Series, 1572(1). https://doi.org/10.1088/1742-6596/1572/1/012079

20. Sa'adah, U., Himmah, S. W., Suprayogi, T., Diantoro, M., Sujito, S., & Nasikhudin, N. (2019). The effect of time deposition of Pan/TiO2 electrospun on photocurrent performance of dye-sensitized solar cell. Materials Today: Proceedings, 13, 175–180. https://doi.org/https://doi.org/10.1016/j.matpr.2019.03.210
21. Sethi, D., & Sakthivel, R. (2017). ZnO/TiO2 composites for photocatalytic inactivation of Escherichia coli. Journal of Photochemistry and Photobiology B: Biology, 168, 117–123. https://doi.org/https://doi.org/10.1016/j.jphotobiol.2017.02.005
22. Subalakshmi, K., & Senthilselvan, J. (2018). Effect of fluorine-doped TiO2 photoanode on electron transport, recombination dynamics and improved DSSC efficiency. Solar Energy, 171, 914–928. https://doi.org/https://doi.org/10.1016/J.SOLENER.2018.06.077
23. Wei, L., Wang, P., Yang, Y., Dong, Y., Fan, R., Song, W., Qiu, Y., Yang, Y., & Luan, T. (2017). Enhanced performance of dye sensitized solar cells by using a reduced graphene oxide/TiO2 blocking layer in the photoanode. Thin Solid Films, 639, 12–21. https://doi.org/https://doi.org/10.1016/j.tsf.2017.08.011
24. Zatirostami, A. (2021). A dramatic improvement in the Efficiency of TiO2-based DSSCs by simultaneous incorporation of Cu and Se into its lattice. Optical Materials, 117. https://doi.org/10.1016/j.optmat.2021.111110